Developments and applications of discontinuum modelling to rock engineering

Giovanni Barla, Marco Barla
Department of Structural and Geotechnical Engineering, Politecnico di Torino, Italy

Masantonio Cravero
CNR, Torino, Italy

Corrado Fidelibus
Università di Taranto, Italy

ABSTRACT: The paper is to discuss the role of discontinuum modelling in rock engineering. This modelling procedure is more frequently used at present than in the past, when continuum modelling was nearly the only method adopted for design analysis. This trend is favoured by the advances in computational methods, which make it possible to use both 2D and 3D simulations of discontinua. Also important is the increased ability in the identification and quantification of design parameters for both the single element (intact rock and discontinuities) and system behaviour (jointed rock mass). Examples are taken from case studies in tunnelling and rock slopes, when the problem is to assess the stability conditions. Also considered is the role of discontinuum modelling in the study of flow through jointed rock masses.

1. INTRODUCTION

The use of computer-based numerical methods for the design analysis of rock engineering problems has been growing steadily over the past few decades. One reason for this is the gradual increase of interest of specialists in numerical methods toward the development of techniques and tools applicable to specific engineering problems in geomechanics. Another reason is the recognition by practitioners of the advantages which can be gained in dimensioning complex engineering structures by the adoption of these methods.

As the interest was moving toward an improved description of rock mass behaviour, the most effort was devoted initially to the developments and applications of methods for the analysis of continuum and equivalent continuum problems. While specialized equations and criteria were being derived and validated for the description of joint strength and deformability, discontinuum modelling was getting a growing attention in view of the solution of problems in practical situations, although continuum modelling continues to be to date the most frequently applied method. It is the aim of this paper to underline the advantages which can be gained by the use of discontinuum modelling in rock engineering practice.

2. TUNNEL ENGINEERING

The prediction of the rock mass response to the excavation of a tunnel is a complex engineering problem. The interest at the design analysis stage is to assess the stability conditions of the excavation in the “intrinsic state” (i.e. when no support/stabilization measures are installed) and when methods of tunnel excavation/construction and support are adopted.

The key of this process is the level of understanding achieved in describing the rock mass conditions (in terms of geological, geomechanical, in situ stress and hydrogeological parameters) and the ability to account for the fundamental components of rock mass behaviour, by using appropriate methods for the analysis of stresses and deformations in the rock mass around the tunnel and in its structural components (pre-support/pre-stabilization measures; primary and final support, etc.).

A number of methods are available for the stress analysis of tunnels, from the earliest closed-form solutions to the most recent numerical modelling methods. With the computational power today available at a reasonable cost, it is possible to solve increasingly sophisticated problems. In particular, with the advent of numerical methods, we have assisted to the development of techniques which have been conceived to model realistically the rock mass behaviour. This is quite different from the early start of geomechanics, when the methods of analysis and the solutions used were mostly taken from other engineering disciplines.

If we restrict our attention to numerical modelling methods and rigorous analysis of tunnelling problems, two procedures are applicable as follows:

- Equivalent continuum: the rock mass is treated as a continuum with equal in all directions input data for the strength and deformability properties, which define a given constitutive relation for the medium: elastic, elasto-plastic, etc.

- Discontinuum: the rock mass is represented as a discontinuum and most of the attention is devoted to the characterization of the rock elements and discontinuities (including major discontinuities and joint systems).

2.1 Continuum modelling

The use of continuum modelling in tunnel engineering makes it essential to simulate the rock mass response to excavation by introducing an equivalent continuum. The most common way to solve this problem, which seems to have gained wide acceptance, is to scale the intact rock properties down to the rock mass properties by using the empirically defined relations given by Hoek & Brown (1997). The next step is the adoption of the appropriate constitutive relations for the rock mass.

A number of computer-based numerical methods have been developed over the past few decades and provide the means for obtaining appropriate solutions to tunnel engineering problems in the framework of the equivalent continuum approach. Among the most frequently used methods are the finite element (FEM), the finite difference (FDM) and the boundary element (BEM) methods, as recently reviewed by Gioda and Swoboda (1999).

2.2 Discontinuum modelling

With the understanding that rock joints and discontinuities in a rock mass play a key role in the response of a tunnel to excavation (joints can create loose blocks near the tunnel profile and cause local instability; joints weaken the rock mass and enlarge the displacement zone caused by excavation; joints change the water flow in the vicinity of the excavation, Shen & Barton 1997), the use of discontinuum modelling has been gaining increasing attention in tunnel engineering.

As recently reviewed by Kawamoto & Aydan (1999), problems involving discontinuum modelling by numerical methods can be solved to a full extent by the distinct element method (DEM) and discontinuum deformation analysis (DDA). In particular, the first method as implemented in the UDEC and 3DEC codes is frequently being applied to tunnel engineering. However, it is to be recognized that discontinuum modelling in general is not being used for design analysis of tunnels as extensively as continuum methods and is considered to be a relatively “new” and “not yet proven” numerical method for design analysis.

2.3 Discussion

Accordingly, when investigating a particular problem at the design analysis stage in tunnel engineering the decision is to choose between continuum and discontinuum modelling of rock mass behaviour. This may be based on the analysis of the likely mechanisms (sliding along joints, opening of joints, block rotation and movement, etc.) which may influence the tunnel stability and the joint spacing relative to the size of the excavation. Consideration may be given to a suggested range of Q-values for which discontinuum modelling will be more appropriate than continuum modelling - $Q \cong 0.1 - 100$ (Barton 1998).

The use of numerical modelling in engineering practice, connected with the need to adopt modelling schemes (continuum versus discontinuum modelling) which are the most appropriate in order to analyse a given problem (provided that sufficient data are available), points out that "the modelling of the components, rock, rock joints and discontinuities is far more logical and relevant than present black box continuum models" (Barton 1999). The comparison shown in Figure 1 well demonstrates this point of view, especially if critical mechanisms of the physical problem under study are to be included in the analysis.

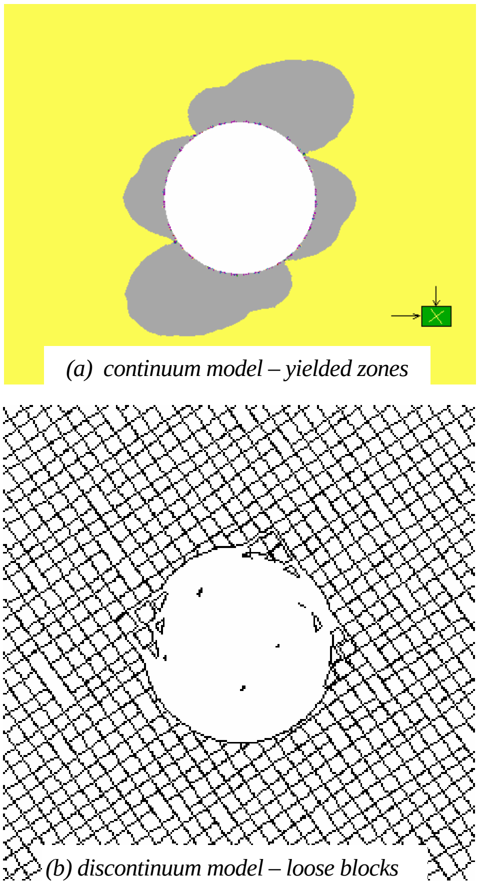
(a) continuum model – yielded zones

(b) discontinuum model – loose blocks

Figure 1. Comparison of (a) continuum ubiquitous joints and (b) discontinuum modelling results when analysing typical instability mechanisms around a TBM excavated tunnel in a weak rock mass.

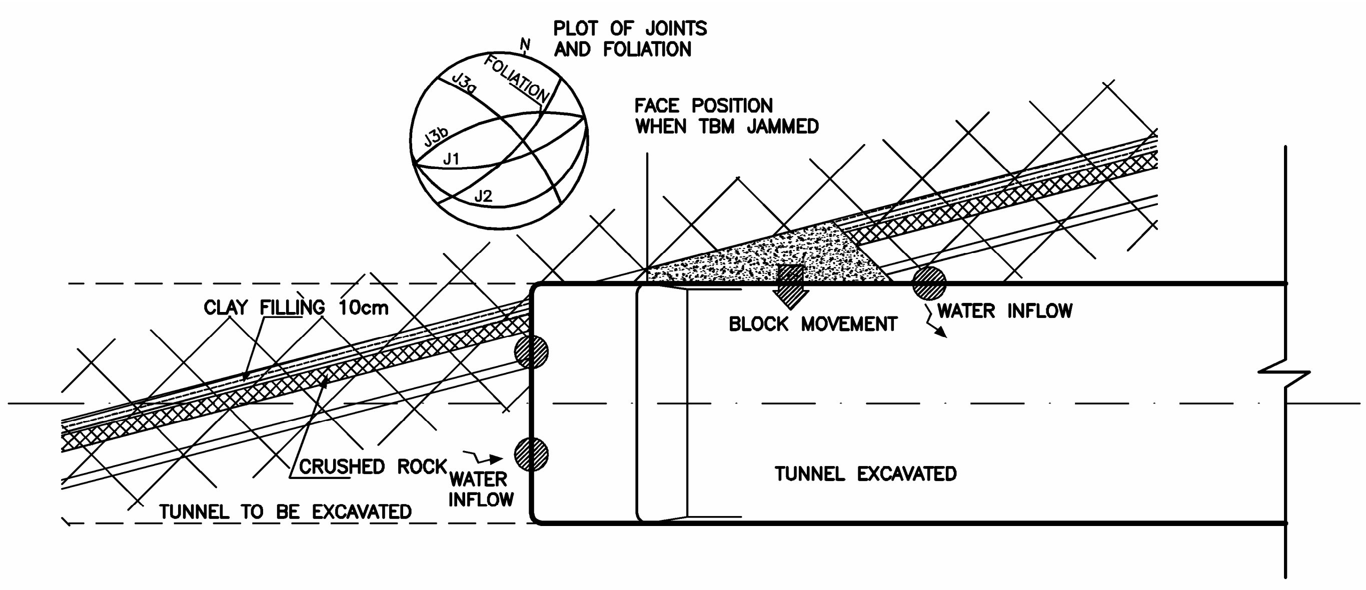

Figure 2. Sketch of the rock conditions at the face (plan view).

There is a relevant question which arises with reference to the use of discontinuum modelling in tunnel engineering and rock engineering, in general. This is in relation to the complexity of the discontinuum model to be used in order to be certain that the critical structural features have not been left out of the analysis (Hart 1993). From one side, the difficulty is in providing sufficient geological data; from the other side, the computer hardware requirements may exceed that available.

Based on the experience gained so far, a possible approach to this problem consists in using discontinuum modelling in connection with rock mass classification methods in a framework of cross-validation of the expected tunnel response to excavation. Once the specific model has been proven to be acceptable in a given rock mass condition, it may be improved and further validated during tunnel excavation. A set of guidelines, given as a function of Q values, can be used as a form of preliminary verification of a numerical model (Barton 1999).

2.4 Case example

2.4.1 Background information

The case study considers the crossing of a fault zone in a TBM excavated tunnel in the Susa Valley, near Torino (Italy). This tunnel (4.75 m diameter) is being excavated by an open TBM configuration through quartzitic micaschists under a cover which is to reach 800 m maximum. The sketch shown in Figure 2 gives a simplified illustration of the conditions at the tunnel face where the TBM became temporarily stuck as a consequence of overstressing and a 25 cm block movement of the right sidewall (Figure 3).

The quartzitic micaschists, which have been extensively tested both in the laboratory and in situ (Barla et al. 1999), are characterized by the presence of three to four joint systems including foliation. Based on geological mapping once the TBM could drill a few meters ahead of the section where it jammed, at least two sub-parallel discontinuities could be evidenced, the second of which (a fault with strike N66E and dip 83° to the S, which intercepts the tunnel axis) has a clay filling and gouge with aperture ranging from a few centimeters to more than a decimeter.

Figure 3. Photograph showing the head of TBM jammed with rock overstressing and block movement of the right sidewall.

The rock mass conditions were estimated on a 7 m tunnel length, with RMR index equal to 31. According to a more complete Q-logging estimate due to Barton (1997), an extreme range of Q-values of about 0.007 ("exceptionally poor" - locally) to 0.3 ("poor") showed a weighted mean of all recordings of about 0.05. Water is flowing through the joints at a temperature of 20°. No quantitative data have been recorded of the water pressure, which seems unlikely to be exceeding, with an overburden of 650 m, a maximum of 6 to 7 MPa (outside the tunnel drainage area).

2.4.2 Discontinuum modelling

With the understanding that discontinuities (major discontinuities and jointing) play a key role in the development of tunnel instability, the problem was investigated by adopting discontinuum modelling, with the 2D distinct element code, UDEC. The rock mass surrounding the tunnel was represented by two discontinuous models as follows.

2.4.3 Deterministic model

The rock mass was considered to be intercepted by three sets of joints, and foliation. Different spacing, degree of persistence and shear strength properties were introduced in the model so as to simulate the rock mass conditions away from the fault zone as illustrated in Figure 4. The joints were assumed to be Mohr-Coulomb joints, i.e. elasto-perfectly plastic joints. The blocks were treated as elasto-plastic material which follows Mohr-Coulomb criterion. The properties of rock blocks and joints are listed below:

Material Properties		Zone (Figures 4 and 5) 1	2	3
E_m	[GPa]	60	30	10
ν_m	[-]	0.25	0.35	0.35
c	[MPa]	34	6.0	2.8
ϕ	[°]	38	36	34

c = cohesion; ϕ = friction angle; E_m = Young's modulus; ν_m = Poisson's ratio.

Joint Properties		Zone (Figures 4 and 5) 1	2	3	Joint (Figures 4 and 5) 1 - 2
K_n	[GPa/m]	40	5×10^{-3}	10×10^{-3}	1.25×10^{-3}
K_s	[GPa/m]	4	5×10^{-4}	10×10^{-4}	1.25×10^{-4}
c	[MPa]	0.1	0	0	0
ϕ	[°]	33	22	22	22

K_n, K_s = normal and shear stiffness; c = joint cohesion; ϕ = joint friction angle.

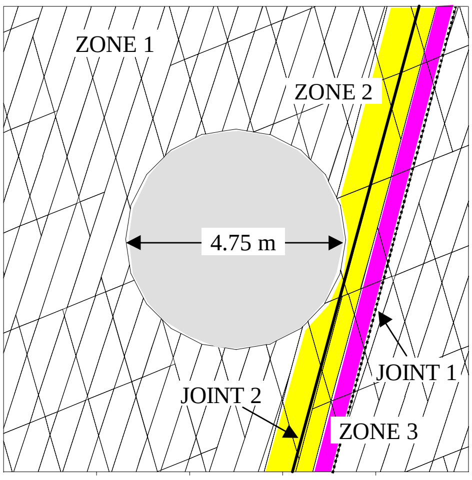

Figure 4. Detail of UDEC deterministic model showing regions with different material and joint properties.

2.2.4 Discrete Feature Network (DFN) model

A Discrete Feature Network (DFN) model was also created by using the procedures implemented in the FracMan code (Dershowitz et al. 1995). The results of geological mapping on the right wall of the tunnel formed the basis for defining the input data in terms of orientation, size and degree of fracturing for the joint sets J1, J2 and J3 a, b. These were superimposed with foliation and discrete features represented by the two sub-parallel discontinuities described above.

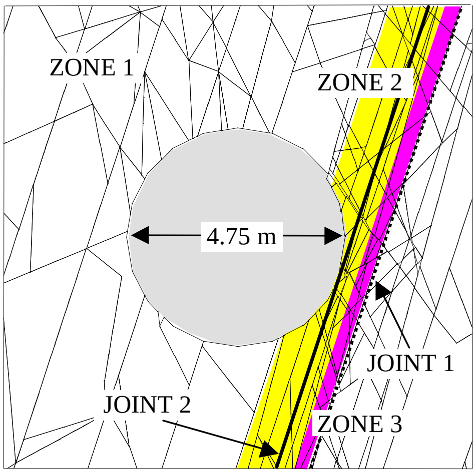

Figure 5. Detail of UDEC-DFN model showing regions with different material properties and joints.

The UDEC model was obtained by taking a cross section orthogonal to the tunnel axis through the 3D DFN volume. This network of 2D fractures is not directly amenable to UDEC analysis as the fractures need to be well connected and no isolated fractures can be handled by the code. At the same time, it was necessary to cross-validate the model against the rock mass conditions around the tunnel. This was carried out by increasing the block size in the original 2D network model both at the crown and on the left wall, to account for the generally better rock mass conditions in these zones.

A random process which cancels the fracture traces exceeding a given limit-length fixed was used in conjunction with the Set edge command which is available with the UDEC code. A typical model finally developed is shown in Figure 5. As for the deterministic model described above, the joints were assumed to behave as Mohr-Coulomb joints and the blocks were treated as elasto-plastic material. The input data are the same as listed above.

2.4.5 Results

The analysis were carried out for both the deterministic and discrete feature network models as shown in Figures 4 and 5 by simulating full face excavation without any support (i.e. in the intrinsic state). The initial state of stress in the model was taken to be as follows (Barla et al. 1999):

σ_1 = maximum principal stress = 21 MPa
σ_2 = minimum principal stress = 4.2 MPa
θ_1 = angle of σ_1 with respect to the vertical axis = 15°.

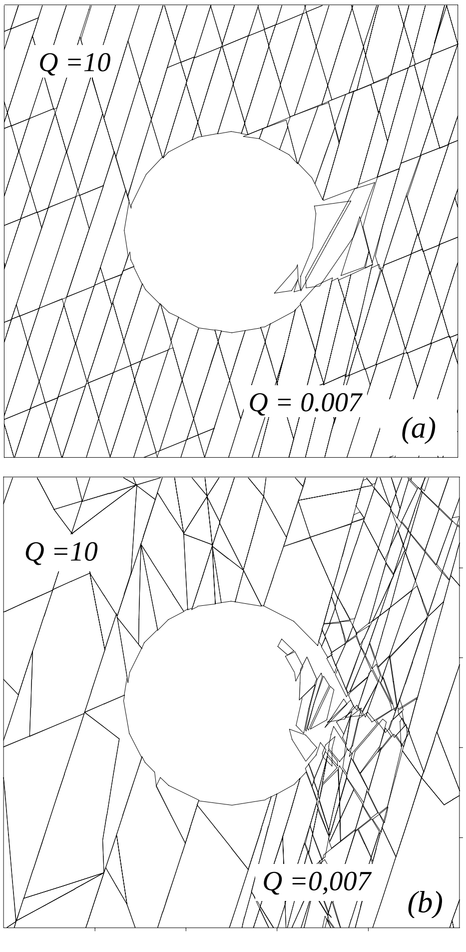

Figure 6. Block movements around the tunnel; (a) deterministic model, (b) DFN model.

The results obtained are plotted in Figure 6 a, b by showing the block movements around the tunnel. It is observed that both the deterministic and discrete feature network model capture well the overstressing conditions of the right wall of the tunnel. If one compares this pattern of behaviour with the actual conditions observed in the tunnel, the remarkable similarity is the block movement developing on the right wall, whereas stable conditions are experienced along the periphery away from the fault zone at the crown and left wall.

4. SLOPE ENGINEERING

Rock slope stability covers a vast area in geomechanics from geological, geomorphological and hydro-geological characterization to the assessment of strength-deformability properties of the rock mass and discontinuities at different scale. Of great relevance are both the understanding of external forces (i.e. groundwater influence, seismicity, external loading) and stabilization measures (i.e. drainage, reinforcement, anchoring, etc.) when applied in order to prevent and/or control instability from developing.

If the interest is centered on the identification of potential failure mechanisms, one is to look for modelling procedures which allow for the understanding of the in situ conditions and potential development of such conditions as function of the key parameters determining stability. However, modelling should not be created with the intention of simulating failure according to a preconcieved mechanism, although it need be recognized that the identification and analysis of failure modes (i.e. toppling failure, plane and wedge sliding failure, footwall buckling failure, etc.) still remains a very useful tool for the study of stability conditions of rock slopes (Hoek & Bray 1981, Sharp 1996).

By restricting to modern numerical modelling methods, one should recognize once again that he has the option to choose between equivalent continuum and discontinuum procedures, as already emphasized with reference to tunnel engineering. However, when dealing with rock slopes, the importance of discontinuities and description of their characteristics in controlling the relevant physical and mechanical processes points out the role of discontinuum modelling.

3.1 Continuum Modelling

The use of continuum modelling in slope engineering leads to the representation of the constitutive equations of the rock mass comprised of the discontinuities and rock material properties by using the empirical equations given by Hoek and Brown (1997) in order to obtain the rock mass properties of the equivalent continuum. However, great care is required, as clearly stated by the proponents of such equations: even rock masses which appear to be good candidates for the application of equivalent continuum modelling may be intercepted by discontinuities controlling stability conditions.

Continuous formulations based on FEM and FDM methods should therefore be considered restrictive in their applicability to the analysis of rock slopes. However, there are obvious cases where, to some extent, these methods are applicable, in particular when use is made of joint and interface elements which are available with them.

3.2 Discontinuum Modelling

The capability of discontinuum modelling to correctly simulate the behaviour of the rock mass, including the discontinuity response, and, to some extent, the interactive coupling of slope and hydraulic response, makes it ideal for design analysis of rock slopes, provided that adequate input data from field are obtained. Based on currently available numerical codes, this implies the use of discrete element codes such as UDEC.

As for the case of application in tunnel engineering, also for slopes the use of discontinuum modelling is complex in terms of the input data and experience gained in the analytical representation of physical processes. Perhaps, it is fair to say that to some extent one is forced into a position of implicit trust in the model (Sharp 1996). At the same time, there are obvious limitations as the analyses predict the stress-deformation responses of both the blocks and discontinuities, and are not able to study overall equilibrium and incorporate specific failure modes.

3.3 Discussion

The option of using continuum or discontinuum modelling of rock mass behaviour for design analysis of rock slopes is available. As already observed, the application of continuum representations in the case of rock slopes need to incorporate in the model the major discontinuities, in order to allow discrete displacements to occur along them.

If the input data are available, in terms of the representation of all salient geological structures, including rock joint systems, there is an obvious implication in using discontinuum modelling for a better representation of rock slope problems. The case of a very high cut shown in Figure 7, with an overall height of about 120 m, gives a clear indication of the advantages gained by using discontinuum modelling compared with continuum modelling, although incorporating the influence of major geological structures (Barla et al. 2000).

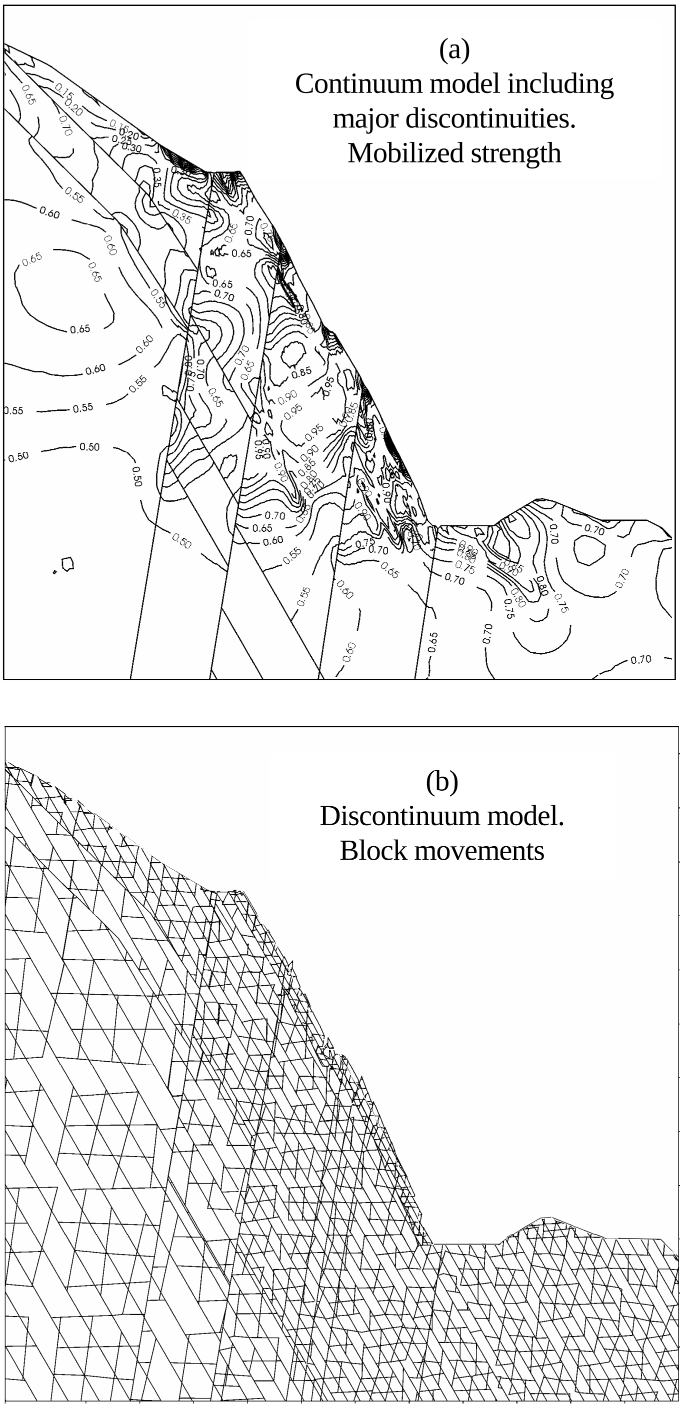

Figure 7. Comparison of (a) continuum model and (b) discontinuum model results when analysing the instability modes of a high rock cut in a limestone rock mass.

3.4 Case example

3.4.1 Background information

On November 5, 1994, during the severe rainfall event which hit the Piemonte and Liguria regions in northern Italy, a plane shear slope instability occurred near the town of San Raffaele Cimena (Torino), with dramatic consequences as shown in Figure 8. The slope movements occurred by translational sliding and resulted in collapse of houses and loss of lives (Barla et al. 1998).

The landslide covers a total area of 4000 m^2, with a volume of mobilized rock (sandy marl and weak sandstone layers) estimated to be in the range of 20000 m^3. The instability resulted in sliding of rock blocks with movement down-dip along the bedding. The dip of the bedding planes in the area ranges from 15° to 20°, with a dip direction of 250°-270°.

Figure 8. Aerial photograph showing the San Raffaele Cimena landslide site. Also shown is the trace of the E-W cross section given in Figure 9.

Plane shear instabilities at the site are essentially governed by the unfavourable orientation of the bedding planes, which occur nearly parallel to the slope surface, and the shear strength properties of these same planes. In the case under study the translational failure took place on one sliding plane down-dip along the beddings. This was clearly ascertained based on the investigations undertaken following the event which included detailed geological mapping and drilling of boreholes in the sliding area and in the near surrounding. As illustrated in Figure 9, the most likely plane of shear failure, dipping at 18° to the West, could be inferred.

Two additional factors could be shown to have an important influence on the plane shear slope instability:

1) undercutting at the toe of the slope, associated with the lateral release of the down-dipping bedding planes, due to a road cut running from the top down, in the landslide area;

2) the exceptionally heavy rainfall event which determined a significant rise of the groundwater table within the slope, also favoured by the inability of the drainage system of the house complex uphill to avoid water to flow down-slope without control.

Laboratory tests were conducted on rock material and discontinuities, including saw-cut surfaces and bedding planes. The samples for testing were obtained from cores and included fine grained sandy marl and weak sandstone (Barla et al. 1998). The direct shear tests on sawcut surfaces taken from sandy marl and weak sandstone gave the basic friction angle to be in the range from 30° to 33°, with the minimum value holding true for marl. A limited number of tests could be conducted on the bedding planes with the normal stress ranging between 0.1 and 1.0 MPa. These tests in

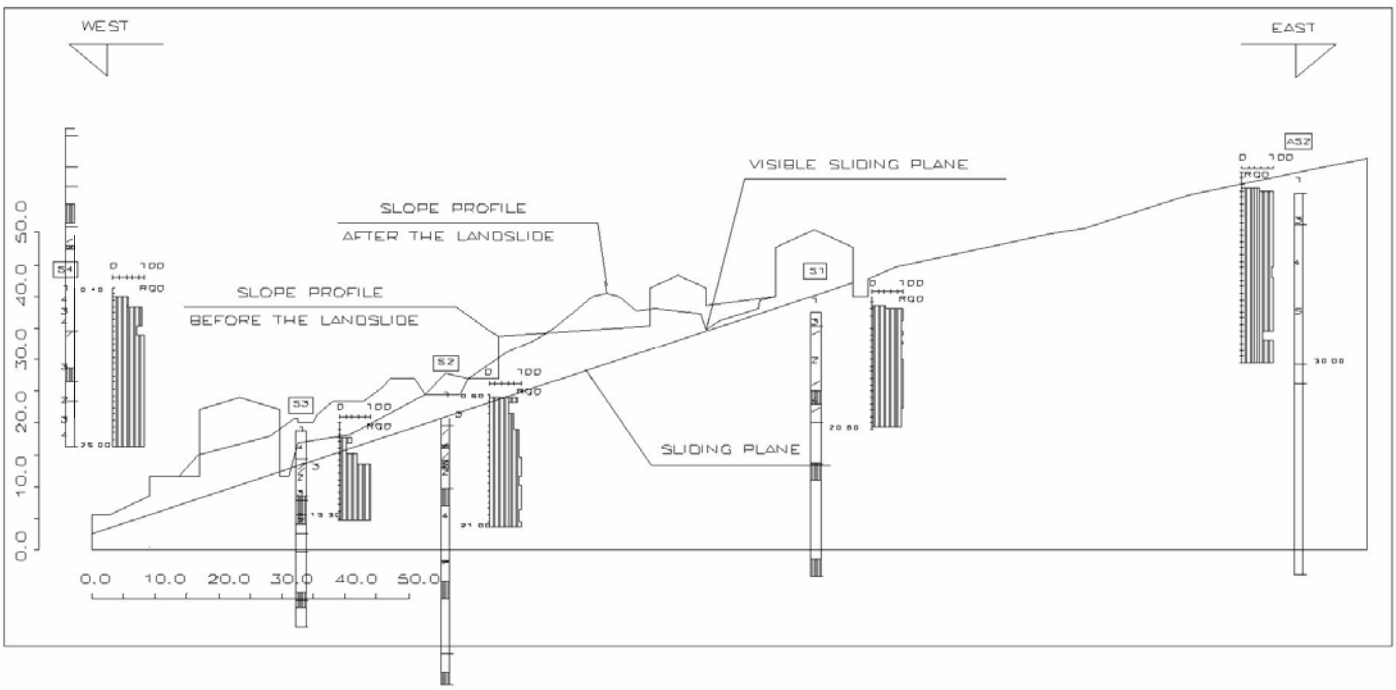

Figure 9. San Raffaele Cimena landslide: E-W cross section through the landslide area showing the plane of shear failure and the slope profiles prior and subsequent to the landslide.

two cases involved discontinuities which did not undergo any previous displacement, whereas in three cases these clearly pertained to the sliding plane (the tests were conducted on samples taken from rock blocks and cores near the sliding plane): the residual friction angle was found to be 22°.

3.4.2 Discontinuum modelling

With the main purpose to investigate the instability phenomenon a study was undertaken with the use of numerical modelling. The distinct element method (DEM) was adopted to simulate the weak discontinuum and computations were performed with UDEC. The E-W cross section of Figure 9 was taken as representative of the slope, with the purpose to simulate both the conditions prior and subsequent to the shear plane instability. As shown in Figure 10 a, the slope section was discretized into rectangular blocks subdivided by the bedding planes and subvertical joints.

The rock blocks were modelled as linear elastic and isotropic. The shear behaviour of the discontinuities (bedding planes and subvertical joints) was modelled by using the continuously yielding option which is available in the UDEC code in order to simulate a shear stress-shear strain curve of the softening type. To this end the Joint Initial Friction (JIF) and Joint Roughness (JIR) parameters were as shown in the table below, where also given are the other parameters used in the analyses.

Material Properties		Discontinuity Properties		
			Bedding planes	Subvertical Joints
E_m [GPa] =	2.0	ϕ_r [°] =	22	22
ν_m [-] =	0.25	JIF =	0.62	0.62
c [MPa] =	0.5	JIR [m] =	0.001	0.001
ϕ [°] =	40	K_n [GPa/m] =	8	8
		K_s [GPa/m] =	0.8	0.8

where: E_m = Young's modulus, ν_m = Poisson's ratio, c = cohesion of intact material, ϕ = friction angle of intact material, ϕ_r = joint residual friction angle, JIF = joint initial friction parameter, JIR = joint roughness parameter, K_n = normal stiffness along joint, K_s = shear stiffness along joint.

Modelling was performed by considering two different geometrical conditions for the slope:

(a) model with no cut in the toe zone;
(b) model with cut in the toe zone.

In each case the following computational steps were considered:

(1) consolidation under self-weight loading, to reach an initial equilibrated configuration;
(2) water head in the rock discontinuities;
(3) iterative analysis, to reach a final configuration.

The interest was centered on the influence of the water head in the rock dicontinuities by assuming this to change from 50, 70 per cent water head up to full saturation.

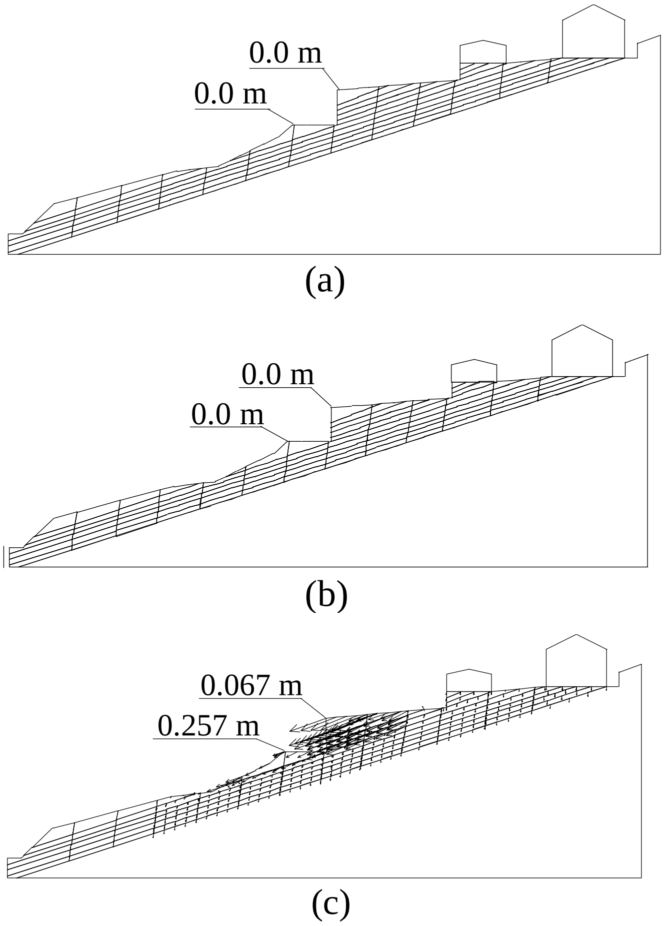

Figure 10. UDEC results showing block translational sliding along the slope. No cut in the toe zone; simulated conditions of: (a) 50 per cent, (b) 70 per cent, (c) 100 per cent water head.

3.4.3 Results

The results obtained for cases (a) and (b) above are illustrated in Figures 10 and 11 by plotting the displacement vectors of rock blocks along the slope.

It is clear from Figure 10 that, with the water head in excess of 70 per cent above the sliding plane and with no cut in the toe zone, some form of instability develops only on the upper layers of the slope, with a maximum displacement down-slope of the order of 0.257 m, when a full saturation condition is simulated. This trend of behaviour motivated the analysis of translational sliding by introducing the effect of undercutting at the toe zone, with simulated conditions of 70 per cent water head.

One may observe from Figure 11 a to c that in this case the instability phenomenon is initiated at the toe and develops up-slope progressively. As shearing occurs along the bedding planes, the subvertical joints open and block sliding takes place. This type of behaviour reproduces well the actual conditions in the field. It is relevant to remark that shearing penetrates at the depth of 5 m at the toe, as direct consequence of the slope cut and absence of passive reaction.

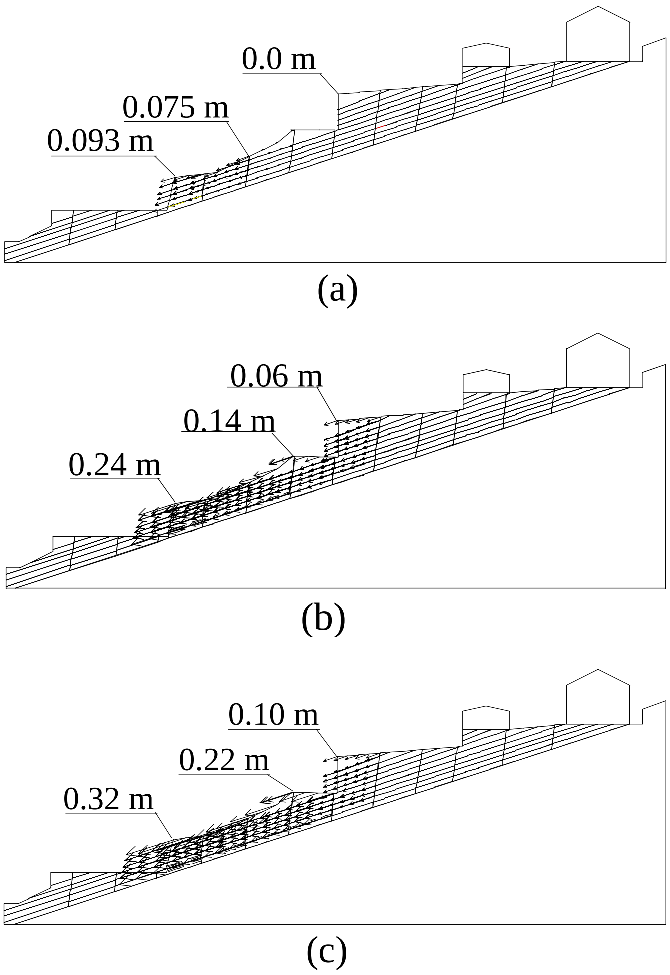

Figure 11. UDEC results showing progressive block translational sliding along the slope. Cut in the toe zone; simulated conditions of 70 per cent water head.

4. HYDRAULIC BEHAVIOUR OF JOINTED ROCK MASSES

The analysis of the hydraulic behaviour of jointed rock masses implies the study of fluid flow through joints, which requires an appropriate understanding and modelling of joint network characteristics. This understanding is linked directly, in hydrologic and transport problems, to geo-structural exploration at given scales and borehole testing for joint transmissivity, along with the interpretation and synthesis of the pertinent joint parameters. Joint modelling and flow analysis should be carried out by joint system models (Dershowitz and Einstein, 1988).

A joint system model should be able to reproduce the essential features of natural jointing, i.e. major disjunctive structures (faults, shear zones, …) and medium to small size joints. Although the hydraulically effective branches of a joint system could be a small portion of the geometrical system itself, this results from a connectivity or a flow analysis performed on the whole joint network. Having established that the joint network is the fundamental precursor of any flow analysis, rules must be followed in order to construct a synthetic joint network (SJN). A class of joint network simulators is of the stochastic-geometric type, which requires the parameters of the joint location process and distributional forms for joint attitude, size, and transmissivity. Correlation among parameters and functional relations with depth can also be introduced (Dershowitz 1992).

The generated joint model statistically conforms to the characteristics of the actual joint network and reflects lack or evidence of spatial correlation. Other rules can be derived from the knowledge of the genetic processes and allow grouping of joints coming from a single deformation event. A structural trend can also be reproduced by iterating geometrical transformations giving raise to a fractal pattern (Hobbs 1976). Furthermore, jointing style, emerging from a genetic-mechanical process can be used as an indirect improvement for the stochastic-geometric modelling, in the sense that a hierarchical dependence between joints is allowed by generating primary and higher order joint sets (Barton 1995).

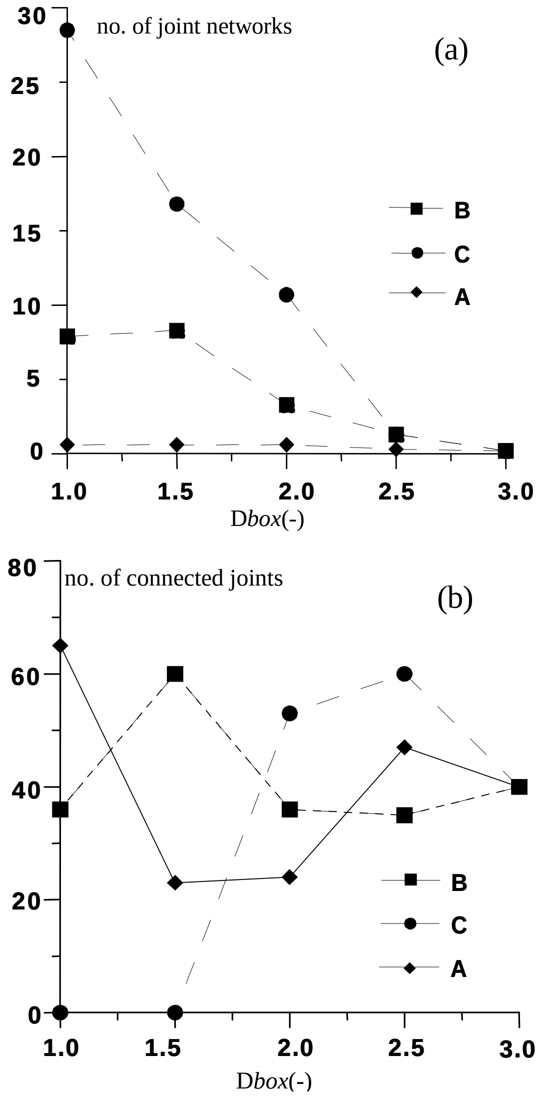

Figure 12. (a) number of joint networks; (b) number of joints directly or indirectly connected to a vertical borehole 50 m long

(A=S1, S2 Poisson, S3Dbox; B=S1 Poisson, S2, S3 Dbox; C=S1, S2, S3 Dbox).

SJN modelling and analysis offer important insights into the 3D parameters of jointing evidently linked to water flow, like the number of independent networks (no. of networks) in a given joint pattern and the total number of joints directly or indirectly connected to a borehole (no. of connected joints). Figure 12 (obtained by means of some FracMan realizations of a joint system made of three strictly orthogonal joint sets: S1 horizontal, S2 trending NS, S3 WE) shows the trend of the two parameters above when the location process of joint centers is changed from pure Poisson to fractal box having different strength of clustering. All the other joint set parameters (joint radius=15 m, joint intensity 0.1 m^2/m^3 for each one set) are constant for all the realizations.

The synthetic joint network that is the output of stochastic-geometric simulators is only one of the possible realizations coming from populations of random variables. In this sense a SJN collects the intrinsic variability of the rock mass jointing and the answers from just one SJN cannot be conclusive about the hydraulic behavior of the joint system. The analyses should explore more than one rock mass picture, and this can be accomplished by a Monte Carlo procedure.

4.1 Hydrologic model

A SJN can be submitted to flow analysis provided the transmissivity parameter and storativity (when unsteady flow is considered) are given to each joint. The flow model is purely hydrological when the flow regime and the volumetric deformation of the jointed rock mass, accompanying the pressure variation of the fluid, are uncoupled. In this hypothesis the flow regime is described by the diffusion equation. In the general 3D case the SJN is very complex and even 100000 or more significant joints must be modelled when an aquifer has to be analyzed. The resulting computational task could be not practicable, especially when flow analyses are part of a stochastic simulation procedure involving several realizations of the SJN. These technical aspects are crucial and different solution schemes have been provided using FEM or BEM.

Apart from the relative merits of the different schemes, some forms of simplifying assumptions need be introduced when very large SJN are considered. The following three categories of approximations can be handled: the equivalent porous medium (EPM); the stochastic continuum medium (SCM); the equivalent pipe network (EPN). All these methods provide a consistent reduction of the computational effort. The application of the first method depends on the existence of a representative elementary volume (REV), based on one or more generated networks. The other two are in general applicable but introduce a certain degree of approximation.

4.2 Examples of SJN in flow and pollutant analyses

Two purely explanatory examples using the SJN concept for flow and pollutant analyses are described in the following. Both examples refer to a cubic domain (1km edge), confined by an impermeable formation except for the N & S sides, where a 10 m hydraulic head is applied (Figure 13). A 100 m deep well P is located in the middle of the domain, with a steady state discharge of 1 l/s. The SJN is made of 4 joint sets, generated according to the parameters given below:

	no. joints	ϑ_m	φ_m	ϑ_{st}	φ_{st}	L_1	L_2	T_m
1	200	0.	80.	1.	1.	700.	700.	1.e+06
2	400	45.	10.	5.	5.	50.	50.	1.e+05
3	400	135.	5.	5.	5.	50.	50.	1.e+05
4	400	45.	50.	5.	5.	50.	70.	5.e+05

φ_m, ϑ_m(°) average plunge, azimuth of the pole, φ_{st}, ϑ_{st} standard deviation; L_1, L_2 (m) average sides of the rectangular joints, T_m(m^2/s) average transmissivity

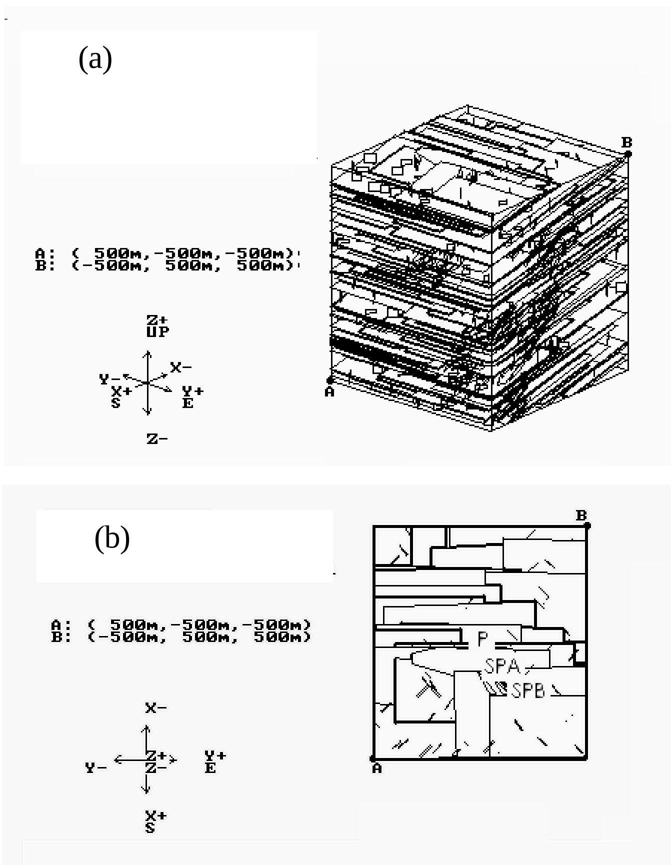

Figure 13. View of a SJN in the cubic domain (a); plan showing the well P and boreholes SPA and SPB (b).

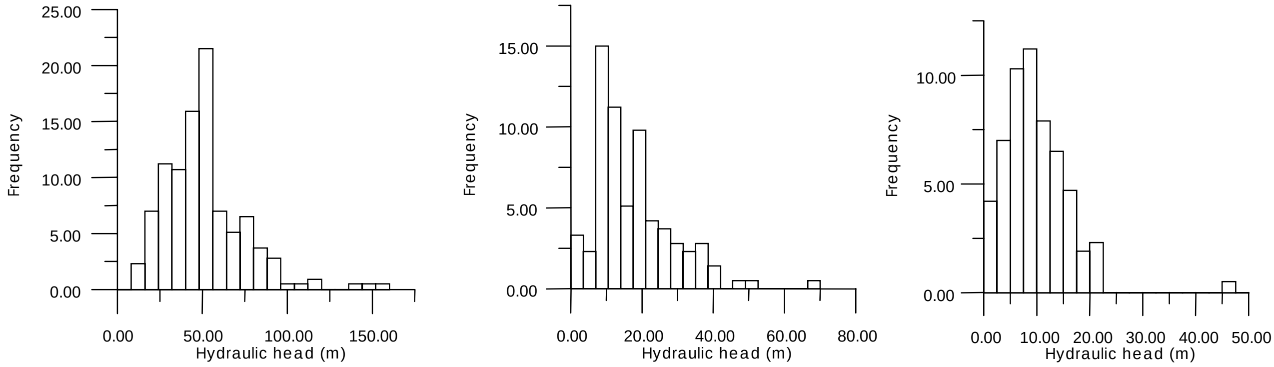

(a) (b) (c)

Figure 14 Variation of the hydraulic head (m) in comparison to the hydrostatic condition, for the well P (a) and the boreholes SPA (b) and SPB (c).

Joint attitude (mean θ_m, φ_m) is bivariate normal. The joints have rectangular shape, with lognormally distributed edges L_1, L_2 (standard deviation 1/10 of the mean size) and the location process of the 3 first sets is Poisson, being the fourth set fractal with a density of 1.5. Transmissivity also is lognormal with standard deviation 1/10 of the mean value.

4.2.1 Case example 1

This case example deals with the appraisal of the steady state heads observed in the central well P and in two 20m deep boreholes, located 100 m (SPA) and 200 m (SPB) apart from the well. A simulation consisting of 200 SJN realisations, carried out with MAFIC (Miller et al. 1995), allows the frequency histograms (Figure 14) of the hydraulic head variations to be obtained in comparison to the hydrostatic condition. SPB is not connected to the well 43% of the time, SPA 35%, while the central well is not connected to the head boundaries 3% of the times, being the average head variations 49.4 m for the well, 11.5 m for SPA and 5.6 m for SPB.

The asymmetry shown by the histograms, where the classes below the mode show higher frequencies, can be explained by the presence of the fractal joint set. Namely in absence of this set one can reasonably expect an almost symmetric behaviour around the mean. On the contrary the fractal set produces joint clusters that, in most cases, act favourably improving the connectivity among joints and a greater rock mass permeability. In other words the isolated clusters have no effect on water percolation, whereas the connected clusters increase the percolation efficiency of the whole joint system: the net effect is the histogram asymmetry.

4.2.2 Case example 2

With the second example, the intent is to evaluate the pollution potential at the well when the borehole SPA releases, for 7 days, 0.01 l/s containing 10 g/l of pollutant. The pollution analysis (particle tracking or purely convective approach - Foxford et al. 1997) refers to a one month period of production at the well and only 15 cases from the fully connective SJN's have been chosen. The sample is small but this evaluation was made only for demonstration purposes. The flow pattern used is that of the steady state solution and the result of the pollutant concentrations at the well for the 15 models is given in Figure 15.

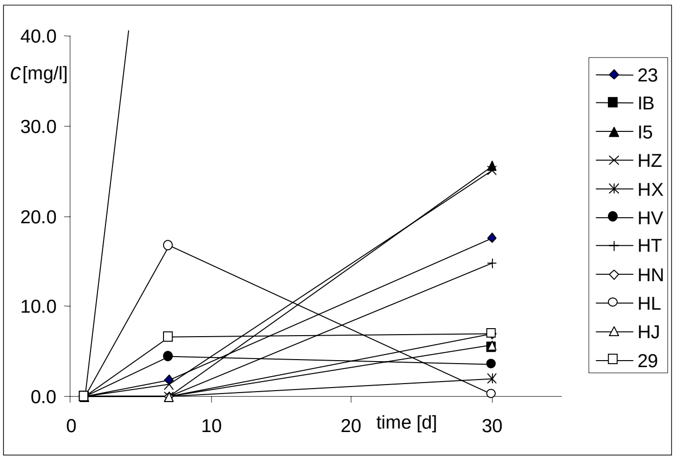

Figure 15. Pollutant concentration *c* (mg/l) versus time at the production well P.

It is noted that the concentration values reflect the variability of the geometrical properties of the joint system, that delays or anticipates the convective flow of pollutant according to the joint connectivity. The network IB (the trend is not entirely represented) conveys 80 mg/l after 7 days to the well. This anomalous behaviour probably depends on the interposition among the pollutant source SPA and the production well of a cluster of conductive joints.

Also to note is that the quality of the results depends on the reliability of the fracture data and that the model predicts a variability of the response that a porous-like medium conceptualization would not be able to show.

5. CONCLUDING REMARKS

This paper has endeavoured to discuss the importance of discontinuum modelling as a design analysis aid in rock engineering. Following a presentation of the issues faced when applying this modelling procedure to tunnel engineering, slope engineering and analysis of the hydraulic behaviour of jointed rock masses, case examples were briefly discussed. These were intended to show the merits of discontinuum modelling in rock engineering practice by describing the differences in the level of information which can be gained by the use of discontinuum representations of rock mass, in particular if compared with continuum modelling.

The use of a model which accounts for the essentially discontinuous nature of the rock mass in engineering design analysis has the great advantage that one need to consider the components of its real behaviour (rock blocks and discontinuities), including the coupling with ground water conditions. This is a consequence of the increased ability to describe the rock mass as a discontinuum from the geometrical, physical and mechanical points of view. It is not to say that equivalent continuum modelling should be ruled out: there are cases where there is no valid substitute to it, as for the analysis of overstressed and weak rock masses. Also, if used with judgement, continuum modelling with the inclusion of discrete features, such as major discontinuities, is essential for comparative calibration of discontinuum modelling results, in the understanding of the overall response of the engineering structure being analysed.

14. REFERENCES

Barla G., Barbero M., Castelletto M. & Maderni G. 1998. A case of plane shear slope instability during the severe rainfall event of 4-6 November 1994 in Piemonte (Italy). *2nd International Symposium on Hard Soils and Soft Rocks, Naples (Italy), 12-14 October 1998*.

Barla G., M. Barla & L. Repetto 1999. Continuum and discontinuum modeling for design analysis of tunnels. *9th Int. Congr. on Rock Mechanics, Paris (France), 25-28 August 1999*.

Barla G., M. Barla, U. Rabagliati, L. Repetto 2000. Reprofiling of a high rock cut slope following instability. *To be published.*

Barton, C. C. 1995. Fractal analysis of scaling and spatial clustering of fractures. *Fractals in the Earth Sciences*. C. C. Barton & P. R. La Pointe eds., Plenum Press.

Barton N. 1997. Pont Ventoux Hydropower Project. Tunnel F2 - Pont Ventoux. Assessment of geological conditions and required support for ch 2350-4000. Report to Nocon. 25 October 1997.

Barton N. 1998. Quantitative description of rock masses for the design of NMT reinforcement (Special Lecture 1*). Int. Conf. on Hydro Power Development In Himalayas, Shimla (India) 1998*.

Barton N. 1999. General report concerning some 20th century lessons and 21st century challenges in applied rock mechanics. *9th Int. Congr. on Rock Mechanics, Paris (France), 25-28 August 1999*.

Dershowitz W. S. 1992. Interpretation and synthesis of discrete fracture orientation, size, shape, spatial structure and hydrologic data by forward modelling. *ISRM Int. Conf. on Fractured and Jointed Rock Masses, Lake Tahoe (CA-USA), 1992*.

Dershowitz, W., G. Lee, J. Geier, T. Foxford, P. LaPointe & A. Thomas 1995. *Interactive discrete fracture data analysis, geometric modelling, and exploration simulation*. User documentation, version 2.5, Golder Associates Inc.

Dershowitz W.S. & H.H. Einstein 1998. Characterizing rock joint geometry with joint system models. *Rock Mechanics and Rock Engineering*, 21, 21-51.

Foxford, T., E. Sudicky, W. Dershowitz, D.A. Shuttle & T. Eiben 1997. *PaWorks, pathways analysis and solute transport*. User documentation, version 1.4. Golder Associates Inc.

Gioda G. & G. Swoboda 1999. Developments and applications of the numerical analysis of tunnels in continuous media. *Int. J. Numer. Anal. Meth. Geomech.*, 23, 1393-1405.

Hart R.D. 1993. An introduction to distinct element modeling for rock engineering. *Comprehensive Rock Engineering*. Volume 2. Analysis and Design Methods (Hudson J.A., editor). 245-263. Pergamon Press, Oxford (UK).

Hobbs B.E., W.D. Means & P.F. Williams 1976. *An outline of structural geology*. Wiley Int. Ed.

Hoek E. & J.W. Bray 1981. *Rock slope engineering*. 3rd Edn. Institute of Mining and Metallurgy. London.

Hoek E. & E.T. Brown 1997. Practical estimates of rock mass strength. *Int. J. Rock Mech. Min. Sci*. Vol. 34, 1156-1186.

Kawamoto T. & O. Aydan 1999. A review of numerical analysis of tunnels in discontinuous rock masses. *Int. J. Numer. Anal. Meth. Geomech*., 23, 1371-1391.

Miller, I., G. Lee, W. Dershowitz & G. Sharp 1995. *MAFIC, matrix/fracture interaction code with solute transport*. User documentation, version b1.5, Golder Associates Inc.

Sharp J.C. 1996. Present understanding and predictive capability of the stability conditions for very high rock cuts. *Eurock '96, Turin (Italy).* Special lectures, Vol. 3.

Shen B. & N. Barton 1997. The disturbed zone around tunnels in jointed rock masses. *Int. J. Rock Mech. Min. Sci*. Vol. 34, pp. 117-125.